SUMMARY OF FINDINGS FROM A USGS SCIENTIFIC INVESTIGATIONS MAP (SIM) AT 1:500k OF THE AEOLIS DORSA REGION, MARS. D. M. Burr[1,2], R. E. Jacobsen[1], A Lefort[1], R. M. Borden[1], and S. E. Peel[1], [1]*at time of research* University of Tennessee, [2]*presently* Northern Arizona University (Devon.Burr@nau.edu)

Introduction: The global dichotomy boundary on Mars commonly exhibits sedimentary materials, as well as volcanic lithologies [1]. The sedimentary units give evidence of geologic and conditions during their formation, such as deltaic deposition [2] and aeolian abrasion [e.g., 3 and refs. therein]. In addition to evidence for extrinsic processes, the dichotomy shows evidence for the intrinsic processes of tectonism [e.g., 4], and volcanism [e.g., 5], and collapse [e.g., 6],.

A series of transitional units, formerly the Medusae Fossae Formation [7], extends along the southern Cerberus and Amazonis margins (~140° E. to ~220° E). Within these transitional units, the Aeolis Dorsa are a population of sinuous ridges between -10.30 N and -8.130 N and 148.60 and 156.520 E (https://planetarynames.wr.usgs.gov), interpreted as extensive fluvial deposits [8-19], exposed by the pervasive aeolian erosion. This substantial record of varied fluvial activity is located ~750 kilometers eastward of Gale Crater, the site of the Mars Science Laboratory [20], and ~950 kilometers eastward of the Interior Exploration using Seismic Investigations, Geodesy and Heat Transport (InSIGHT) mission [21]. Thus, AD provides contextual data for both missions.

To provide this context and decipher the encapsulated climate transition in the AD region, a more complete understanding of the series of geologic processes that sculpted this area was needed. Thus, a 1:500k USGS SIM was created and is in press.

Geography: The map region was designed to focus on the inverted fluvial deposits, concentrated around the interior margins of Aeolis Planum to the west and Zephyria Planum to the east (fig. 1). Between these two plana is a broad (~150-200-km-wide) interplana trough containing the longest of the inverted fluvial deposit, Aeolis Serpens [12]. To the south of the trough is an elongate depression, Aeolis Chaos, up to ~1 kilometer lower than the surroundings. The southwestern map corner exhibits southern highlands terrain. This map area, from -8° to 0 N. and 147.5° to 156° E. long., covers a total area of 230,000 km^2. Named craters include Asau (25 km dia.), Kalba (14 km dia.), Neves (22 km dia.) and Obock (14 km dia.).

Base Map and Data: The basemap for this work, used to establish consistent and salient unit characteristics, was comprised of mosaiced optical images from the Context Camera (CTX; [22]). Secondary datasets were topographic data from the Mars Orbiter Laser Altimeter (MOLA; [23]) and local digital elevation models created using Ames Stereo Pipeline [24 and refs. Therein] from CTX-stereo pair images. Images from the High-Resolution Imaging Science Experiment [25] were used to discern relative stratigraphic relationships and to corroborate unit delineation. Lastly, day- and nighttime infrared data from the Thermal Emission Imaging Spectrometer [26] as a 100-meter/pixel mosaic, were used locally to correlate map unit contacts based on thermal properties. Observations in these secondary data sets supported the derivation of the accompanying Correlation of Map Units (CMU) and additional characteristics in the Description of Map Units (DMU). A blended CTX mosaic [27] was used in map publication due to its improved visual appearance.

Methodology: Our approach follows that of the Planetary Geologic Map Coordination Group [28,29].

Units and Groups. We defined 19 geologic units based on morphologies/landforms, thermal properties, and geographic and/or stratigraphic relationships. Units were grouped into six unit groups (fig. 2).

Feature Types. We mapped a single location feature of <1-km-diameter craters and nine linear features, including ridges (2 types), troughs (2), scarp crests (1), depression margins (1), and crater rims (3).

Age Determinations: Because of the highly erosive landscape [e,g., 3], age determinations (fig. 2) are based on relative stratigraphic and adjacency relationships. Map unit assignments to Martian epochs are extrapolated from previous assignment of the southern highlands units to the Late Noachian epoch.

Geologic Summary: The geologic summary from the USGS SIM is shown pictorial in the CMU (fig. 2).

Noachian Period. The recorded geologic history of the Aeolis Dorsa region begins in the Middle Noachian with the highlands plateau unit (Nhp) emplacement. Broad linear grooves indicate extension, whereas scattered wrinkle ridges point to localized contraction. Semi-rectilinear mesas on Aeolis Plana (Npm) are interpreted as distal plateau outcrops. Further north, hummocky terrain (Nph), perhaps modified highlands, forms a broad ridge across the interplana trough.

Hesperian Period. In the Late Noachian and the Hesperian, the southern-most highlands plateau unit (Nhp) was altered to form the proximal highland mesas unit (HNhm). This weathering also generated the undivided unit (HNhu), visible as talus slopes around plateau margins. Weathering, long-distance transport, and emplacement of plateau materials led to formation of transition terrain units (HNtt and Htu). The chaotic morphology of the transitional chaos terrain unit (Htct)

and negative relief indicates formation by collapse and/or tectonic extension [30].

Repeated aeolian and fluvial sedimentation and erosion occurred throughout the Hesperian. The earliest fluvial deposits were emplaced by meandering rivers (Had_1) that, in the southeastern area of the map, may have terminated in deltas [13] or standing water [18,19]. A second fluvial episode is recorded in the middle Aeolis Dorsa unit (Had_2), and two plana units (AHp_2, Hp_1) are also dated to the Late-Hesperian. A final Aeolis Dorsa unit ($AHad_3$) is expressed as alluvial fans. Deltaic processes are suggested by interpretation of a limited number of these $AHad_3$ deposits as having deltaic planforms, context, and stratigraphy [13]. An undivided Aeolis Dorsa unit (Had_u) is ascribed to the Hesperian period. An interplana mounds unit (Him), stratigraphically interleaved with Aeolis Dorsa units, is interpreted as remnants of plana. Wrinkle ridges indicate localized contraction.

Amazonian Period. Some of the geologic units that originated in the Hesperian period continued to be emplaced or modified during the Early Amazonian, including the fluvial activity of the last Aeolis Dorsa unit ($AHad_3$) and impact cratering reflected in the crater unit (AHc). Aeolian activity is evidenced by the plana units (AHp_2 and AHp_u), which show very sparse crater densities suggestive of recent (or on-going) modification by aeolian erosion. Shallow depressions with few or no small impact craters on both Plana suggest very recent or ongoing aeolian deflation.

Acknowledgments: We thank the USGS Astrogeology Planetary Geologic Map Coordination Group for assistance, Sharon Wilson and Lauren Edgar for constructive reviews. This work was accomplished with funding from the NASA Mars Data Analysis Program and University of Tennessee Graduate Assistantships to REJ, RMB, and SEP.

References: [1] Tanaka K. L. et al. (2014) *USGS SIM* 3292. [2] Di Achille G. and Hynek B. M. (2010). *Nat. Geo., 3,* 459-463. [3] Mandt K. et al., (2009) *JGR 113*, E12. [4] McGill G. E. and Dimitriou A. M. (1990) *JGR 95*, 12595-12605. [5] Hartmann W. K. and Berman, D. C. (2000) *JGR 105*, E6, 15011-15026. [6] Skinner J. A. and Tanaka K. L. (2018). *USGS SIM* 3389. [7] Tanaka K. L. et al. (2005) *USGS SIM* 2888. [8].Burr D. M. et al., (2009) *Icarus 200*, 52-76. [9] Burr D. M. et al. (2010) *JGR 115*, E07011. [10] Lefort A. et al. (2012) *JGR 117*, E03007. [11] Lefort A. et al. (2015) *Geomorph. 240*, 121-136. [12] Williams R. M. E. et al. (2013) *Icarus 225,* 308-324. [13] DiBiase, R. A. et al. (2013) *JGR, 118*, 1-18. [14] Kite E. S. et al. (2015) *Icarus 253*, 223-242. [15] Kite E. S. et al. (2015) *EPSL 420*; 55-65. [16] Jacobsen R. E. and Burr D. M. (2016) *GRL 43*, 17, 8903-8911. [17] Jacobsen R. E. and Burr D. M. (2017) *Geosphere 13*, 6. [18] Cardenas B. T. et al. (2017) *GSAB 130,* 3/4, 484-498. [19] Hughes, C. M. et al. (2019) *Icarus 317*, 442-453. [20] Grotzinger J. P. et al. (2012) *SSR 170*, 1-4, 5-56. [21] Banerdt W. B. et al. (2018) *LPS XLVII* Abs 1896. [22] Malin M. C. et al. (2007) IJGRI 112, E05S02. [23] Smith D. E. et al. (2001) *JGR 106,* E10. [24] Beyer R. A. et al. (2018) *ESS 5*, 5, 537-548. [25] McEwen A. S. et al. (2007) *JGR 115*, E05. [26] Christensen P. R. et al. (2004) *SSR 110*. [27] Dickson J. L. et al. (2018) *LPS XLIX* Abs 2480. [28] Tanaka K. L. et al. (2005) *USGS SIM* 2147. [29] Skinner J. A. et al. (2018) Planet. Geol. Map. Protocol, *USGS ASC*. [30] Lefort A. et al. (2015) *Geomoph. 240*, 121-136.

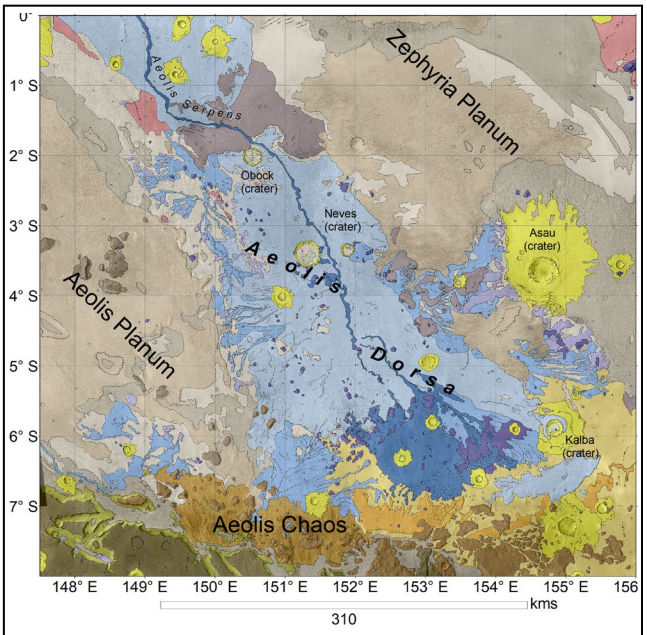

Figure 1: Aeolis Dorsa map, showing geologic units, linear features, and geographic labels. Location features, unit annotations (Fig. 2) omitted for clarity.

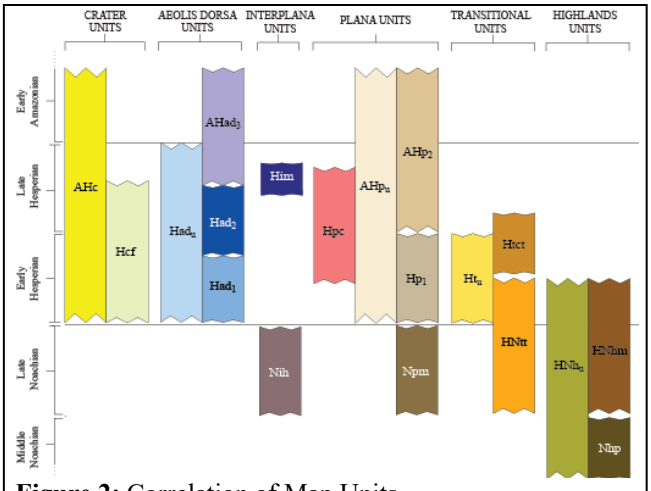

Figure 2: Correlation of Map Units.